

AN ALTERNATIVE SYMBIOTIC CHANNEL TO TYPE Ia SUPERNOVAE

Guoliang Lü^{1,2*}, Chunhua Zhu^{2,3}, Zhaojun Wang^{2,3}, Na Wang¹

¹*National Astronomical Observatories / Urumqi Observatory, the Chinese Academy of Sciences, Urumqi, 830011, China*

²*School of Physics, Xinjiang University, Urumqi, 830046, China*

³*School of Science, Xi'an Jiaotong University, Xi'an, 710049, China*

ABSTRACT

By assuming an aspherical stellar wind with an equatorial disk from a red giant, we investigate the production of Type Ia supernovae (SNe Ia) via symbiotic channel. We estimate that the Galactic birthrate of SNe Ia via symbiotic channel is between 1.03×10^{-3} and $2.27 \times 10^{-5} \text{ yr}^{-1}$, the delay time of SNe Ia has wide range from ~ 0.07 to 5 Gyr. The results are greatly affected by the outflow velocity and mass-loss rate of the equatorial disk. Using our model, we discuss the progenitors of SN 2002ic and SN 2006X.

Key words: binaries: symbiotic—stars: evolution—stars: mass loss—supernovae:general

1 INTRODUCTION

Type Ia supernovae (SNe Ia) are exploding stars which are good cosmological distance indicators and have been used to measure the accelerated expansion of the Universe (Riess et al. 1998; Perlmutter et al. 1999). It is widely accepted that progenitors of SNe Ia are mass accreting carbon-oxygen (CO) white dwarfs (WDs) and they explode as a SN Ia when their masses reach approximately the Chandrasekhar mass (Nomoto et al. 1984). Two families of progenitor models have been proposed: the double-degenerate model and the single-degenerate model. For the double degenerate model, previous works indicated that the expected accretion rates may cause the accretion-induced collapse of the CO WDs and the formation of neutron stars (Nomoto & Iben 1985; Saio & Nomoto 1985). In the single-degenerate model the mass donor is a main sequence (MS) referred to as the WD+MS channel or a red giant (RG) referred to as WD+RG channel (van den Heuvel et al. 1992; Li & van den Heuvel 1997). The latter is also called a symbiotic channel.

According to Han & Podsiadlowski (2004) and Meng et al. (2008), the birth rate of SNe Ia via the WD+MS channel can only account for up to 1/3 of $3 - 4 \times 10^{-3} \text{ yr}^{-1}$ observationally estimated by van den Bergh & Tammann (1991) and Cappellaro & Turatto (1997). Other channels should be important. Recently, Wang et al. (2009) showed that helium star donor channel is noteworthy for producing SNe Ia ($\sim 1.2 \times 10^{-3} \text{ yr}^{-1}$). However, helium associated with SNe Ia fails to be detected (Marion et al. 2003;

Mattila et al. 2005), and Kato et al. (2008) suggested that SNe Ia from helium star donor channel are rare. Therefore, symbiotic channel is a possible candidate. By detecting Na I absorption lines with low expansion velocities, Patat et al. (2007) suggested that the companion of the progenitor of the SN 2006X may be an early RG (However, Chugai (2008) showed that the absorption lines detected in SN 2006X cannot form in the RG wind). Voss & Nelemans (2008) studied the pre-supernova archival X-ray images at the position of the recent SN 2007on, and they considered that its progenitor may be a symbiotic binary. Unfortunately, a WD+RG binary system usually undergoes a common envelope phase when RG overflows its Roche lobe in popular theoretical model. WD+RG binaries are unlikely to become a main channel for SNe Ia. Yungelson et. al. (1995), Yungelson & Livio (1998), Han & Podsiadlowski (2004) and Lü et al. (2006) showed that the birthrate of SNe Ia via symbiotic channel are much lower than that from WD+MS channel. In order to stabilize the mass transfer process and avoid the common envelope, Hachisu et al. (1999) assumed a mass-stripping model in which a wind from the WDs strips mass from the RG. They obtained a high birth rate ($\sim 0.002 \text{ yr}^{-1}$) of SNe Ia coming from WD+RG channel.

Most of previous theoretical works assumed that the cool giant in symbiotic stars shares the same mass-loss rate with field giant and the wind from the cool giant is spherical (Yungelson et. al. 1995; Lü et al. 2006, 2008). However, based on cm and mm/submm radio observations (Seaquist et al. 1993; Mikołajewska et al. 2003) and IRAS data (Kenyon et al. 1988), mass-loss rates for the symbiotic giants are systematically higher than those reported for field giants. Recently, Zamanov et al. (2008) found that

* E-mail: guolianglv@gmail.com (LGL)

the rotational velocities of the giants in symbiotic stars are 1.5–4 times faster than those of field giants. Using the relation between rotational velocity and mass-loss rate found by Nieuwenhuijzen & de Jager (1988), Zamanov et al. (2008) estimated that the mass-loss rates of the symbiotic giants are 3–30 times higher than those of field giants. In addition, O’Brien et al. (2006) suggested that the bipolarity in the 2006 outburst of the recurrent nova RS Oph may result from an equatorial enhancement in its cool giant. If the cool giant in symbiotic star has high mass-loss rate and an aspherical stellar wind, the contribution of symbiotic channel to total SNe Ia may be significantly enhanced.

In this work, assuming an aspherical stellar wind with equatorial disk around the symbiotic giant, we show an alternative symbiotic channel to SNe Ia. In § 2 we present our assumptions and describe some details of the modeling algorithm. In § 3 we show WD+RG systems in which SNe Ia are expected. The population synthesis’ results are given in § 4. Main conclusions are in § 5.

2 PROGENITOR MODEL

For the binary evolution, we use a rapid binary star evolution code of Hurley et al. (2002). When the primary has become a CO WD and the secondary just evolves into first giant branch (FGB) or asymptotic giant branch (AGB), an aspherical wind from the secondary is considered. In other phases of binary evolution, we adopt the descriptions of Hurley et al. (2002).

2.1 Aspherical winds from cool giants in symbiotic stars

In general, the stellar wind from a normal RG is expected to be largely spherical due to the spherical stellar surface and isotropic radiation. However, the majority (> 80%) of observed planetary nebulae are found to have aspherical morphologies (Zuckerman & Aller 1986; Balick 1987). This property can be explained by two models: (i) the generalized wind-blown bubble in which a fast tenuous wind is blown into a previously ejected slow wind (see a review by Frank (1999)); (ii) the interaction of the slow wind blown by an AGB star with a collimated fast wind blown by its companion (Soker 2000). In two models, the slow wind is aspherically distributed and the densest in the equatorial plane. The aspherical wind with an equatorial disk may result from the stellar rotation (Bjorkman & Cassinelli 1993) or a simple dipole magnetic field (Matt et al. 2000). Asida & Tuchman (1995) showed that an anisotropic wind from AGB star can be caused by combining rotation effects with the existence of an inflated atmosphere formed by the stellar pulsation. Therefore, the fast rotation and strong magnetic field are crucial physical conditions for an equatorial disk.

An isolated RG usually has a low rotational velocity so that its effect can be neglected. Furthermore, using a traditional method applied for the solar magnetic field, Soker (1992) estimated the magnetic activity of AGB stars, and found that the level of activity expected from single AGB stars is too low to explain the aspherical wind. However, the situations in symbiotic stars are different. Soker (2002) showed that the cool companions in symbiotic systems are

likely to rotate much faster than isolated RGs due to accretion, tidal interaction and back-flowing material. According to measurements of the projected rotational velocities of the cool giants 9 symbiotic stars and 28 field giants, Zamanov et al. (2008) found that the rotational velocities of the giants in symbiotic stars are 1.5–4 times faster than those of field giants, which confirmed the results of Soker (2002). Stellar magnetic activity is closely related to the rotation. The cool giants with fast rotational velocities are prime candidates for possessing strong magnetic field (Soker 2002). Therefore, the cool giants in symbiotic stars, having the fast rotation velocity and strong magnetic field, can result in aspherical winds. However, in binary systems, the orbital motion, the magnetic field and the gravitational influence of the companions can complicate the structure of the outflow (Soker 1994, 1997; Frankowski & Tylanda 2001). A detailed structure of the winds is beyond the scope of this work. By assuming several parameters, we construct a primary aspherical model to describe the morphology of winds from cool giants in symbiotic stars.

No comprehensive theory of mass loss for RGs exists at present. Hurley et al. (2000) applied the mass loss laws of Reimers (1975) and Vassiliadis & Wood (1993) to describe the mass-loss rates of FGB and AGB stars, respectively. As mentioned in Introduction, the mass-loss rates for the symbiotic giants are systematically higher than those reported for field giants. We use a free parameter ζ to represent the enhanced times of mass-loss rates during FGB and AGB phases for the symbiotic giants by

$$\dot{M}_L = \zeta \dot{M}_{RG} \quad (1)$$

where \dot{M}_{RG} is the mass-loss rate of RG in Hurley et al. (2000).

In the present work, the winds from cool giants in symbiotic stars flow out via two ways: an equatorial disk and a spherical wind. The total mass-loss rate \dot{M}_L is represented by

$$\dot{M}_L = \dot{M}^d + \dot{M}^{\text{sph}} \quad (2)$$

where \dot{M}^d and \dot{M}^{sph} give the mass-loss rates via the equatorial disk and the spherical wind, respectively. We assume that the ratio of the mass-loss rate in the equatorial disk to the total mass-loss rate is represented by a free parameter η , that is,

$$\dot{M}_L = \dot{M}^d / \eta = \dot{M}^{\text{sph}} / (1 - \eta). \quad (3)$$

In this work we make different numerical simulations for a wide range of ζ and η .

The mass-loss rates \dot{M}_L , \dot{M}^d and \dot{M}^{sph} are affected by the rotational velocities and the magnetic activities of the RGs in symbiotic stars. The rotational velocities and the magnetic activities depend on the binary evolutionary history (Soker 2002). In the present paper we focus on the effects of the aspherical wind with an equatorial disk on the formation of SNe Ia. We neglect the different rotational velocities and magnetic activities which result from the different binary evolutionary history and result in different \dot{M}_L , \dot{M}^d and \dot{M}^{sph} . This work overestimates the contribution of the symbiotic stars with long orbital periods to SN Ia. Recently, Soker (2008) suggested the existence of an extended zone above the AGB star where parcels of gas do not reach the escape velocity. In general, the binary with an AGB

star have a long orbital periods. The low outflow velocity of stellar wind greatly increases the efficiency of the companion accreting stellar wind. In our work, we do not consider the extended zone above the AGB star, which results in an underestimate the contribution of the symbiotic stars with long orbital periods to SN Ia. Therefore, it is acceptable for a primary model to neglect the binary evolutionary history and the extended zone above the AGB star.

2.2 Wind accreting

In symbiotic stars WDs accrete a fraction of the stellar winds from cool companions. In the present paper a stellar wind is composed of a spherical wind and an equatorial disk. For the former, according to the classical accretion formula in Bondi & Hoyle (1944), Boffin & Jorissen (1988) gave the mean accretion rate in binaries by

$$\dot{M}_a^{\text{sph}} = \frac{-1}{\sqrt{1-e^2}} \left(\frac{GM_{\text{WD}}}{v_w^2} \right)^2 \frac{\xi_w}{2a^2} \frac{1}{(1+v^2)^{3/2}} \dot{M}^{\text{sph}}, \quad (4)$$

where $1 \leq \xi_w \leq 2$ is a parameter (Following Hurley et al. (2000), $\xi_w = \frac{3}{2}$), v_w is the wind velocity and

$$v^2 = \frac{v_{\text{orb}}^2}{v_w^2}, \quad v_{\text{orb}}^2 = \frac{GM_t}{a}, \quad (5)$$

where a is the semi-major axis of the ellipse, v_{orb} is the orbital velocity and total mass $M_t = M_{\text{hot}} + M_{\text{cool}}$. For the equatorial disk, we neglect the diffusion of equatorial disk, that is, the disk thickness is constant. The accretion rate of WD is relative to the crossing area of its gravitational radius in orbital plane, which is approximately given by :

$$\dot{M}_a^{\text{d}} = \frac{R_G v_{\text{orb}}}{\pi a v_w} \dot{M}^{\text{d}} \quad (6)$$

where $R_G = 2GM_{\text{WD}}/(v_w^2 + v_{\text{orb}}^2)$ is the gravitational radius of WD accretor. If $v_{\text{orb}} \gg v_w$, the accretion rate given by Eq. (6) may be higher than \dot{M}^{d} . It is necessary that the WD does not accrete more mass than that lost by the RG. So we enforced the condition $\dot{M}_a^{\text{d}} \leq 0.9\dot{M}^{\text{d}}$. For $v_{\text{orb}} \ll v_w$, we requested \dot{M}_a^{d} is not lower than $R_g/(\pi a)\dot{M}^{\text{d}}$. Eq. (6) overestimates the contribution of the symbiotic stars with long orbital periods to SN Ia because we neglect the diffusion of equatorial disk. Total mass accretion rate is

$$\dot{M}_a = \dot{M}_a^{\text{d}} + \dot{M}_a^{\text{sph}} \quad (7)$$

Based on Eqs. (4) and (6), accretion rate depends strongly on the wind outflow velocity v_w which is not readily determined. For the spherical winds, we adopt the prescription in Hurley et al. (2002), and $v_w = \sqrt{2\beta_w \frac{GM_{\text{cool}}}{R_{\text{cool}}}}$ where $\beta_w = 1/8$. In general, the equatorial disk has a lower outflow velocity than the spherical wind (Bjorkman & Cassinelli 1993; Asida & Tuchman 1995), and the typical wind velocity of field giant is between ~ 5 and 30 km s^{-1} . Due to the existence of an extended zone above the AGB star (Soker 2008), the outflow velocity of the equatorial disk can be very low. In this work the outflow velocity of the equatorial disk v_w is taken as 2, 5 and 10 km s^{-1} in different numerical simulations.

2.3 Mass transfer rate of Roche lobe overflow

When a secondary overflows its Roche lobe, we assume that there is no equatorial disk for the secondary. At this time the mass transfer via the inner Lagrangian point (L_1) can be dynamically unstable or stable. If the mass ratio of the components ($q = M_{\text{donor}}/M_{\text{accretor}}$) at the onset of Roche lobe overflow is larger than a certain critical value q_c , the mass transfer is dynamically unstable and results in the formation of a common envelope. The issue of the criterion for dynamically unstable Roche lobe overflow q_c is still open. Hjellming & Webbink (1987) did a detailed study of stability of mass transfer using polytropic models. Han et al. (2001, 2002) showed that q_c depends heavily on the assumed mass-transfer efficiency. Recently, Chen & Han (2008) studied q_c for dynamically stable mass transfer from a giant star to a main sequence companion. They found that q_c almost linearly increases with the amount of the mass and angular momentum lost during mass transfer. In this work, for normal main sequence stars $q_c = 3.0$ while $q_c = 4.0$ when the secondary is in Hertzsprung gap (Hurley et al. 2002). Based on the polytropic models in Hjellming & Webbink (1987), Webbink (1988) gave q_c for red giants by

$$q_c = 0.362 + \frac{1}{3 \times (1 - M_c/M)}, \quad (8)$$

where M_c and M are core mass and mass of the donor, respectively. In our work, we adopt the q_c of Webbink (1988).

When $q < q_c$, the binary system undergoes a stable Roche lobe mass transfer and the mass transfer rate is calculated by

$$\dot{M}_L = 3.0^{-6} [\ln(R_d/R_{Ld})]^3 M_{\odot} \text{yr}^{-1} \quad (9)$$

where R_d and R_{Ld} are donor's radius and Roche lobe radius, respectively. Details can be seen in Hurley et al. (2002).

When $q > q_c$, the binaries in which the giants overflow the Roche lobe immediately evolve to the common envelope phase, while the binaries for the main sequence stars overflowing the Roche lobes will undergo the dynamically stable mass transfer.

2.4 Evolution of accreting WD

Instead of calculating the effects of accretion on to the WD explicitly, we adopt the prescription of Hachisu et al. (1999) for the growth of the mass of a CO WD by accretion of hydrogen-rich material from its companion (also see Han & Podsiadlowski (2004); Meng et al. (2008)). If the mass accretion rate \dot{M}_a exceeds a critical value, \dot{M}_{cr} , the accreted hydrogen burns steadily on the surface of the WD at the rate of \dot{M}_{cr} . The unprocessed matter is assumed to be lost from the systems as an optically thick wind at a rate of $\dot{M}_{\text{wind}} = \dot{M}_a - \dot{M}_{\text{cr}}$ (Hachisu et al. 1996). The critical mass-accretion rate is given by

$$\dot{M}_{\text{cr}} = 5.3 \times 10^{-7} \frac{1.7-X}{X} (M_{\text{WD}} - 0.4) M_{\odot} \text{yr}^{-1} \quad (10)$$

where X is the hydrogen mass fraction and is 0.7 in this work. If the mass-accretion rate \dot{M}_a is less than \dot{M}_{cr} but higher than $\dot{M}_{\text{st}} = \frac{1}{2}\dot{M}_{\text{cr}}$, it is assumed that there is no mass loss and hydrogen-shell burning is steady. If \dot{M}_a is between $\frac{1}{2}\dot{M}_{\text{cr}}$ and $\frac{1}{8}\dot{M}_{\text{cr}}$, the accreting WD undergoes very weak hydrogen-shell flashes, where we assume that the processed

mass can be retained. If \dot{M}_a is lower than $\frac{1}{8}\dot{M}_{cr}$, hydrogen-shell flashes are so strong that no mass can be accumulated by the accreting WD. The growth rate of the mass of the helium layer on top of the CO WD can be written as

$$\dot{M}_{He} = \eta_H \dot{M}_a \quad (11)$$

where

$$\eta_H = \begin{cases} \dot{M}_{cr}/\dot{M}_a, & \dot{M}_a > \dot{M}_{cr}, \\ 1, & \dot{M}_{cr} \geq \dot{M}_a \geq \frac{1}{8}\dot{M}_{cr}, \\ 0, & \dot{M}_a < \frac{1}{8}\dot{M}_{cr}. \end{cases} \quad (12)$$

When the mass of the helium layer reaches a certain value, helium is possible ignited. If helium-shell flashes occur, a part of the envelope mass is assumed to be blown off. The mass accumulation efficiency for helium-shell flashes, η_{He} , is given by Kato & Hachisu (2004). Then, the mass growth rate of the CO WD, \dot{M}_{WD} , is

$$\dot{M}_{WD} = \eta_H \eta_{He} \dot{M}_a. \quad (13)$$

When the mass of accreting CO WD reaches $1.378 M_\odot$, it explodes as a SN Ia.

3 WD+RG SYSTEMS IN WHICH SNE IA ARE EXPECTED

In this section, according to the assumptions in the above section, we simulate the evolutions of the binary systems with a CO WD and a MS. All input parameters are the same with those in case 1, that is, the outflow velocity of equatorial disk $v_w = 5 \text{ km s}^{-1}$, $\eta = 0.9$ and $\zeta = 10$. The initial masses of WDs are $0.76, 0.8, 0.9, 1.0, 1.1,$ and $1.2 M_\odot$, respectively. The initial orbital periods are from 0.8 to 11000 days with $\Delta \log P^i = 0.1$ days. The initial masses of MSs are between 1.2 and $2.0 M_\odot$ with $\Delta M_2^i = 0.05 M_\odot$ when $\dot{M}_{WD}^i = 0.76 M_\odot$ and $\dot{M}_{WD}^i = 0.80 M_\odot$, between 1.15 and $3.0 M_\odot$ with $\Delta M_2^i = 0.1 M_\odot$ when $\dot{M}_{WD}^i = 0.9 M_\odot$ and $\dot{M}_{WD}^i = 1.0 M_\odot$, between 1.1 and $3.5 M_\odot$ with $\Delta M_2^i = 0.1 M_\odot$ when $\dot{M}_{WD}^i = 1.1 M_\odot$, between 1.0 and $8 M_\odot$ with $\Delta M_2^i = 0.25 M_\odot$ when $\dot{M}_{WD}^i = 1.2 M_\odot$, respectively.

Fig. 1 shows WD+RG binary systems in the initial orbital period-secondary mass ($\log P^i, M_2^i$) plane. Filled symbols give the binary systems in which CO WDs explode eventually as SNe Ia: Filled squares indicate SN Ia explosions during an optically thick wind phase ($\dot{M}_a \geq \dot{M}_{cr}$); filled circles SN Ia explosions during stable hydrogen-shell burning ($\dot{M}_{cr} > \dot{M}_a \geq \frac{1}{2}\dot{M}_{cr}$); filled triangles SN Ia explosions during mildly unstable hydrogen-shell burning ($\frac{1}{2}\dot{M}_{cr} > \dot{M}_a \geq \frac{1}{8}\dot{M}_{cr}$). Crosses show binary systems which undergo common envelope evolution during WD+RG phases, empty squares represent binary systems which experience stable Roche lobe overflows during WD+RG phases, empty circles give binary systems which are detached WD+RG systems. They can produce symbiotic phenomena while they can not explode as SNe Ia. The binary systems which are not plotted can not evolve to WD+RG phases. They either explode as SNe Ia via WD+MS channel, or become WD+dwarf or helium MS systems.

According to Fig. 1, the progenitors of SNe Ia via symbiotic channel are mainly split into left and right regions. The progenitors in the left region have short initial orbital periods. Table 1 shows an example. The sec-

Table 1. An example for the progenitor of SN Ia with a short initial orbital period. The initial mass of the CO WD is $0.8 M_\odot$, the initial mass of the secondary is $1.9 M_\odot$ and the initial orbital period is 1.99 days. The first column gives the evolutionary age. Columns 2, and 3 show the masses of CO WD and the secondary, respectively. The letters in parentheses of column 3 mean the evolutionary phases of the secondary. MS represents the main sequence, HG for Hertzsprung gap. The fourth column shows the orbital period. Column 5 gives the ratio of the secondary radius to its Roche lobe radius. The last column shows the critical mass ratio q_c . All input physical parameters are same with those in case 1.

AGE (10^6 yr)	$M_{WD}(M_\odot)$	$M_2(M_\odot)$	P (Days)	R_2/R_L	q_c
0.0000	0.80	1.90(MS)	1.99	0.373	—
1352.0	0.80	1.90(HG)	1.99	0.813	—
1357.6	0.80	1.90(HG)	1.99	1.001	4
1363.8	1.26	0.70(FGB)	2.21	2.229	0.83
1364.1	~ 1.378	0.55 (FGB)	3.25	2.003	0.86

ondary overflows Roche lobe during Hertzsprung gap. Due to $M_{donor}/M_{WD} < q_c$, the progenitor experiences stable mass transfer. During Roche lobe overflows, the great deal matter of the secondary has been transferred to the CO WD so that the CO WD becomes more massive while the secondary mass decreases. When the secondary evolves to FGB phase, M_{donor}/M_{WD} has been lower than q_c . Therefore the progenitor undergoes a stable mass transfer in FGB phase till CO WD explodes as SN Ia. In the whole process, there is no aspherical wind with equatorial disk from the secondary. The progenitors in the right region have long initial orbital periods so that the secondaries can evolve into AGB phase. Table 2 shows an example. Due to the high mass-loss rate of RG and the high accretion rate of CO WD resulting from an aspherical wind with equatorial disk, the ratio of mass of RG to that of CO WD is lower than q_c when secondary overflows its Roche lobe. Therefore, the binary system undergoes a stable matter transfer until CO WD explodes as SN Ia. In the progenitors with longer initial orbital periods, the secondaries never overflow Roche lobe and the accretion of CO WDs mainly depends on the aspherical wind with equatorial disk.

Compared with the previous work (Hachisu et al. 1999; Han & Podsiadlowski 2004; Meng et al. 2008), the progenitors in the present work have longer initial orbital periods (up to ~ 10000 days) and wider ranges of initial masses of secondaries (from ~ 1.0 to $8 M_\odot$).

4 POPULATION SYNTHESIS

We construct a set of models in which we vary different input parameters relevant to SNe Ia produced by aspherical stellar wind. Table 3 lists all cases considered in the present work.

4.1 Parameters for binary evolution and binary population synthesis

In order to investigate the birth rate of SNe Ia, we carry out binary population synthesis via Monte Carlo simulation technique. Binary evolution is affected by some uncertain

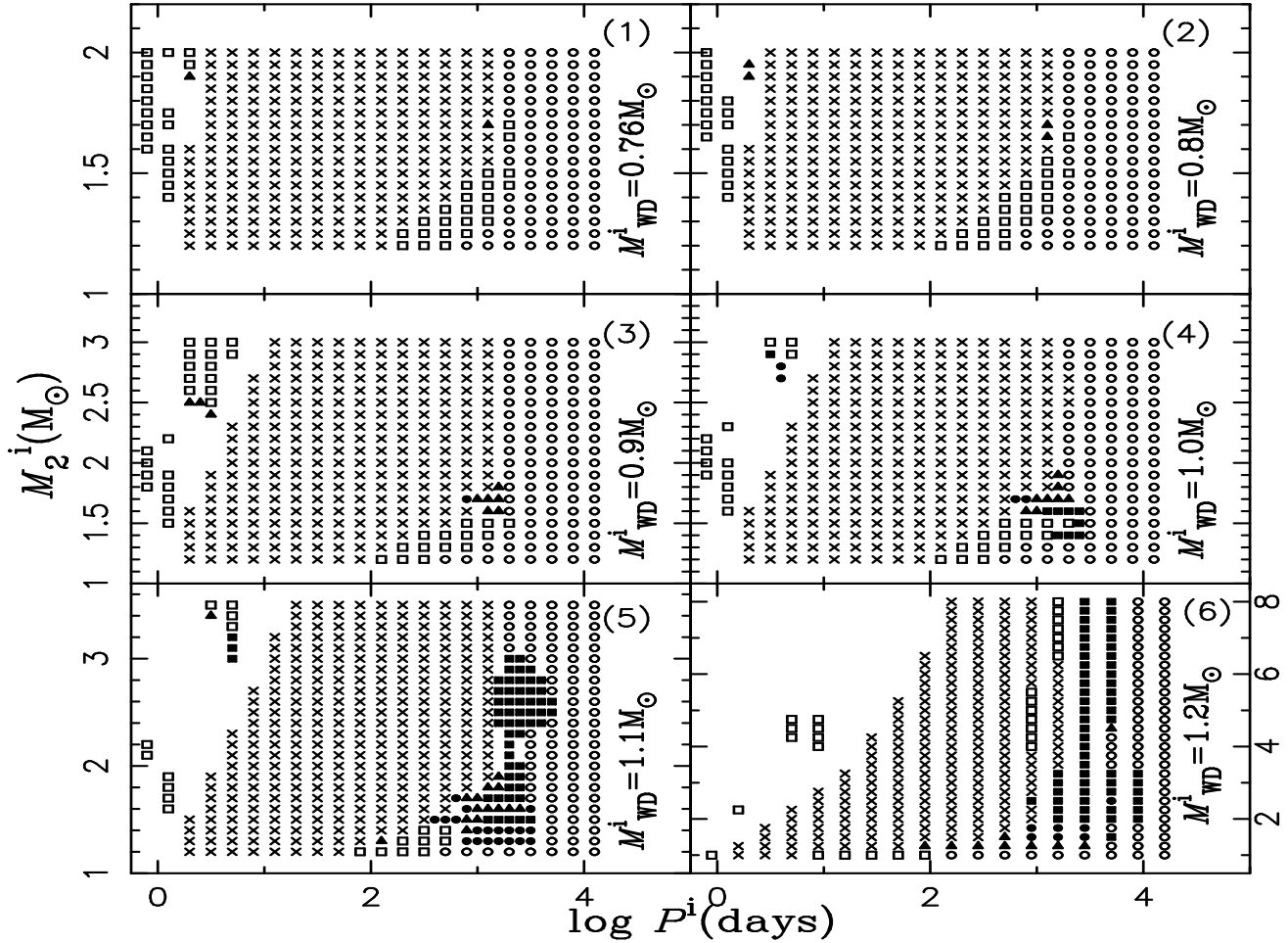


Figure 1. —Final outcomes of the binary evolution in the initial orbital period-secondary mass ($\log P^i, M_2^i$) plane of the CO WD+RG binary, where P^i is the initial orbital period and M_2^i is the initial mass of the donor star (for different initial WD masses as indicated in each panel). Filled squares indicate SN Ia explosions during an optically thick wind phase ($\dot{M}_a \geq \dot{M}_{cr}$), filled circles SN Ia explosions during stable hydrogen-shell burning ($\dot{M}_{cr} > \dot{M}_a \geq \frac{1}{2}\dot{M}_{cr}$), filled triangles SN Ia explosions during mildly unstable hydrogen-shell burning ($\frac{1}{2}\dot{M}_{cr} > \dot{M}_a \geq \frac{1}{8}\dot{M}_{cr}$). Crosses show binary systems which undergo common envelope evolution during WD+RG phase, empty squares represent binary systems which experience stable Roche lobe overflows during WD+RG phase, empty circles give binary systems which are detached systems during WD+RG phase. They can produce symbiotic phenomena while they can not explode as SNe Ia. The numbers along the right y axis in panel 6 only are for $M_{WD}^i = 1.2M_\odot$. Details are in text.

Table 2. Similar to Table 1, but for the progenitor of SN Ia with a long initial orbital period. CHeB means core helium burning. The initial mass of the CO WD is $0.8 M_\odot$, the initial mass of the secondary is $1.7 M_\odot$ and the initial orbital period is 1256 days.

AGE (10^6 yr)	$M_{WD}(M_\odot)$	$M_2(M_\odot)$	P (Days)	R_2/R_L	q_c
0.0000	0.80	1.70(MS)	1256	0.005	—
1873.6	0.80	1.70(HG)	1256	0.010	—
1901.1	0.80	1.70(FGB)	1256	0.014	—
1977.1	0.98	1.33(CHeB)	795	0.064	—
2108.6	0.98	1.30(AGB)	816	0.125	—
2112.3	1.10	1.05(AGB)	666	1.001	1.039
2113.5	~ 1.378	0.55(AGB)	890	1.715	4.64

Table 3. Parameters of the models for SNe Ia via symbiotic channel. The parameter v_w in the second column is the out-flow velocity of equatorial disk. The parameter η in column three gives the ratio of the mass-loss rate in equatorial disk to the total mass-loss rate [See Eq. (3)]. The parameter ζ in the fourth column is the enhanced times of the mass-loss rate during FGB and AGB phases for the secondaries [See Eq. (1)].

Cases	v_w (km s^{-1})	η	ζ
Case 1	5	0.9	10
Case 2	2	0.9	10
Case 3	10	0.9	10
Case 4	5	0.75	10
Case 5	5	0.5	10
Case 6	5	0.25	10
Case 7	5	0.9	5
Case 8	5	0.9	30

input parameters. In this work, the rapid binary star evolution code of Hurley et al. (2002) is used. If any input param-

eter is not specially mentioned it is taken as default value in Hurley et al. (2002). The metallicity $Z=0.02$ is adopted. We assume that all binaries have initially circular orbits, and we follow the evolution of both components by the rapid binary evolution code, including the effect of tides on binary evolution (Hurley et al. 2002).

For the population synthesis of binary stars, the main input model parameters are: (i) the initial mass function (IMF) of the primaries; (ii) the mass-ratio distribution of the binaries; (iii) the distribution of orbital separations.

A simple approximation to the IMF of Miller & Scalo (1979) is used. The primary mass is generated using the formula suggested by Eggleton et al. (1989)

$$M_1 = \frac{0.19X}{(1-X)^{0.75} + 0.032(1-X)^{0.25}}, \quad (14)$$

where X is a random variable uniformly distributed in the range $[0,1]$, and M_1 is the primary mass from $0.8M_\odot$ to $8M_\odot$.

For the mass-ratio distribution of binary systems, we consider only a constant distribution (Mazeh et al. 1992),

$$n(q) = 1, \quad 0 < q \leq 1, \quad (15)$$

where $q = M_2/M_1$.

The distribution of separations is given by

$$\log a = 5X + 1, \quad (16)$$

where X is a random variable uniformly distributed in the range $[0,1]$ and a is in R_\odot .

In order to investigate the birthrates of SNe Ia, we assume simply a constant star formation rate over last 15 Gyr (Han et al. 1995), or a single starburst (Han & Podsiadlowski 2004; Zhang et al. 2005). In the case of a constant star formation rate, we assume that a binary with its primary more massive than $0.8 M_\odot$ is formed annually (Phillips 1989; Yungelson et al. 1993; Han et al. 1995). In the case of a single star burst we assume a burst producing 2×10^7 binary systems in which the primaries are more massive than $0.8 M_\odot$, which gives a statistical error for our Monte Carlo simulation lower than 5 per cent for SNe Ia via symbiotic channel in every case in Table 3.

4.2 Birthrate of SNe Ia via symbiotic channel

Fig. 2 shows the Galactic birthrates of SNe Ia via symbiotic channel. They are between $1.03 \times 10^{-5} \text{yr}^{-1}$ (case 2) and $2.27 \times 10^{-5} \text{yr}^{-1}$ (case 6). Different outflow velocities ($v_w = 2, 5, 10 \text{km s}^{-1}$) of equatorial disk in cases 1, 2 and 3 have a great effect on the birthrates with a factor of ~ 40 . Different ratios of the mass-loss rate in the equatorial disk to total mass-loss rate in cases 1, 4, 5 and 6, η_s ($\eta = 0.9, 0.75, 0.5, 0.25$), give uncertainty of the birthrates within a factor of ~ 9 . Different enhanced times of the mass-loss rate for the symbiotic giants in cases 1, 7 and 8, ζ ($\zeta = 10, 5, 30$), have a weak effect within a factor of 1.6. The observationally estimated the Galactic birthrate of SNe Ia by van den Bergh & Tammann (1991) and Cappellaro & Turatto (1997) is $3 - 4 \times 10^{-3} \text{yr}^{-1}$. In cases 3, 5 and 6, the contribution of SNe Ia via symbiotic channel to total SNe Ia is negligible. However, in case 2 with low outflow velocities ($v_w = 2 \text{ km s}^{-1}$) and

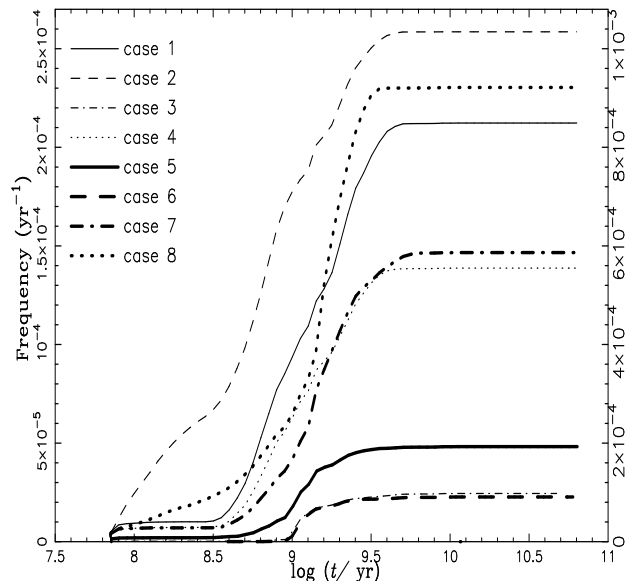


Figure 2. —The evolution of birthrates of SNe Ia for a constant star-formation rate. The key to the line-styles representing different cases is given in the upper left corner. The numbers along the right y axis are only for case 2.

high η ($\eta = 0.90$), the contribution is approximately 1/3, which is comparable with that via WD+MS channel in Han & Podsiadlowski (2004). Our results are greatly affected by the low outflow velocity of equatorial disk and its mass-loss rate.

Fig. 3 displays the evolution of birthrates of SNe Ia for a single star burst of 2×10^7 binary systems. Using observations of the evolution of SNe Ia rate with redshift, Mannucci et al. (2006) suggested that SNe Ia have a wide range of delay time from < 0.1 Gyr to > 10 Gyr. The delay time is defined as the age at the explosion of the SN Ia progenitor from its birth. In the single degenerate scenario, the delay time is closely related to the secondary lifetime and thus the initial mass of the secondary M_2^i (Chen & Li 2007; Hachisu et al. 2008b). In WD+MS channel, Li & van den Heuvel (1997), Han & Podsiadlowski (2004), and Meng et al. (2008) showed that M_2^i is between 2 and $3.5 M_\odot$, which indicates that the range of the delay time is from ~ 0.1 Gyr to 1 Gyr. In order to obtain a wide delay time from ~ 0.1 to 10 Gyr, Hachisu et al. (2008b) assumed that optically thick winds from the mass-accreting CO WD and mass-stripping from the companion star by the WD wind. Assuming an aspherical stellar wind with an equatorial disk from cool giants in symbiotic stars, we give a very wide delay time range from ~ 0.07 Gyr to 5 Gyr. SNe Ia with shorter delay time than 0.1 Gyr result from those progenitors with more massive M_2^i than $\sim 3.5 M_\odot$, SNe Ia with longer delay time than 1 Gyr from those progenitors with lower M_2^i than $2 M_\odot$. Because the delay time determined greatly by the initial mass of the secondary, Fig. 3 can be easily explained by the distribution of the initial masses of the secondaries for SNe Ia in the next subsection.

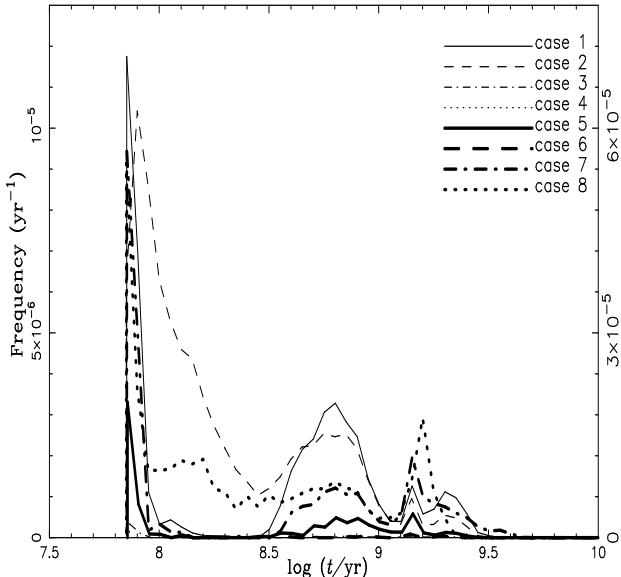


Figure 3.—Similar to Fig. 2, but for a single star burst of 2×10^7 binary systems. The numbers along the right y axis are only for case 2.

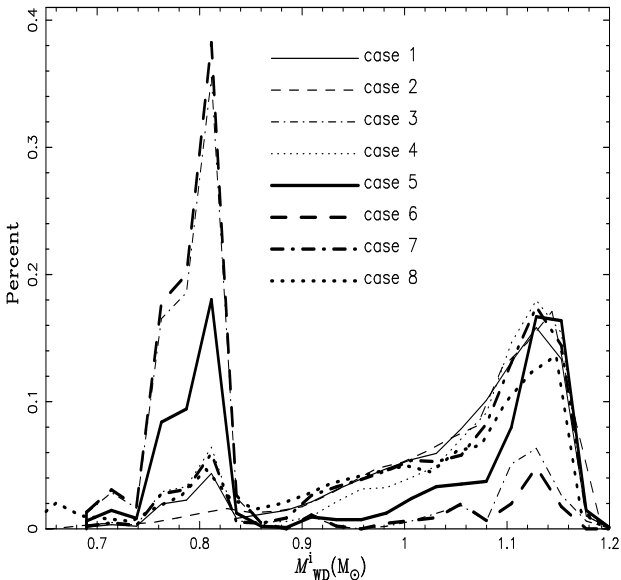


Figure 4.—The distribution of the initial masses of the CO WDs for the progenitors of SNe Ia (the number in every case is normalized to 1 and the width of the bin is $0.03 M_{\odot}$). The cases are indicated in the middle top.

4.3 Distribution of initial parameters

Fig. 4 shows the distribution of the initial masses of the CO WDs that produce ultimately a SN Ia according to our models. There are obviously two peaks. The left peak is at about $0.8 M_{\odot}$, and results mainly from the binary systems with short initial periods like that showed in Table 1 and with long initial periods like that showed in Table 2. The right peak is at about $1.1 M_{\odot}$, and mainly results from binary systems with long initial periods.

Fig. 5 gives the distribution of the initial masses of the

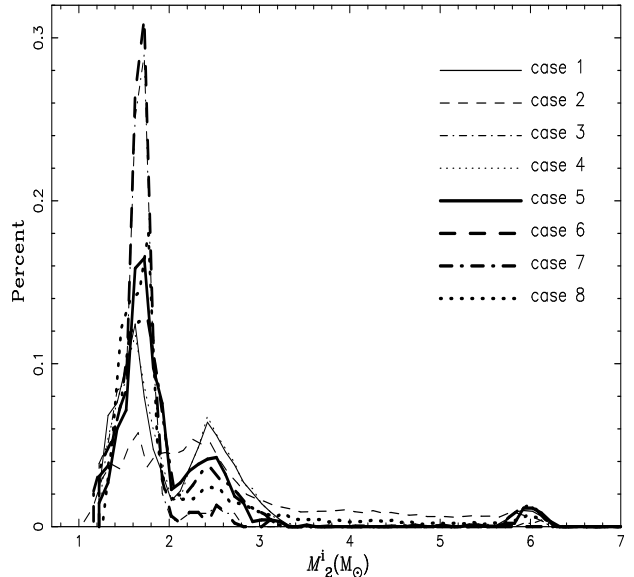


Figure 5.—The distribution of the initial masses of the secondaries for the progenitors of SNe Ia (the number in every case is normalized to 1 and the width of the bin is $0.3 M_{\odot}$). The cases are indicated in the right top.

secondaries for SNe Ia. The distribution shows three regions. The left region is between $\sim 1.2 M_{\odot}$ ($1.0 M_{\odot}$ for case 2) and $\sim 2.0 M_{\odot}$. These SNe Ia have delay time longer than about 1 Gyr and correspond to the right peak of Fig. 3. The middle region is from $\sim 2.0 M_{\odot}$ to $3.0 M_{\odot}$, and results from the progenitors with long orbital periods. These SNe Ia have delay time between ~ 0.5 and 1.0 Gyr and correspond to the middle peak of Fig. 3. The right region is more massive mass than $\sim 3.0 M_{\odot}$. These SNe Ia have very short delay time and correspond to the left peak of Fig. 3. Except case 6, there is a peak at about $6.0 M_{\odot}$ (also see Fig. 6). The peak results from the binaries in which primary initial masses (M_1^i) are more massive than $\sim 5.8 M_{\odot}$, secondary initial masses are between ~ 5.8 and M_1^i , and initial orbital periods are about 10000 days. For these binaries, before the primaries overflow their Roche lobe during AGB phase, the secondaries can accrete some material so that the ratio of primary mass to secondary mass is lower than the critical value q_c . These binaries avoid the common envelope evolution. Then, they have wide binary separations so that the secondaries can evolve RGs and form aspherical stellar winds.

Fig. 6 shows the distributions of the progenitors of SNe Ia, in the “initial secondary mass – initial orbital period” plane. According to Fig. 6, the distribution of the initial orbital periods should have double peaks. The evolution of progenitors with short and long orbital periods can be explained by Tables 1 and 2, respectively. Meng et al. (2008) showed that the distribution of progenitors of SNe Ia via WD+MS channel is between ~ 1 days and 10 days. The orbital distribution via symbiotic channel in this work is much longer than their distribution.

4.4 Progenitor of SN 2002ic

SN 2002ic was the first SN Ia for which circumstellar (CS) hydrogen has been detected unambiguously (Hamuy et al.

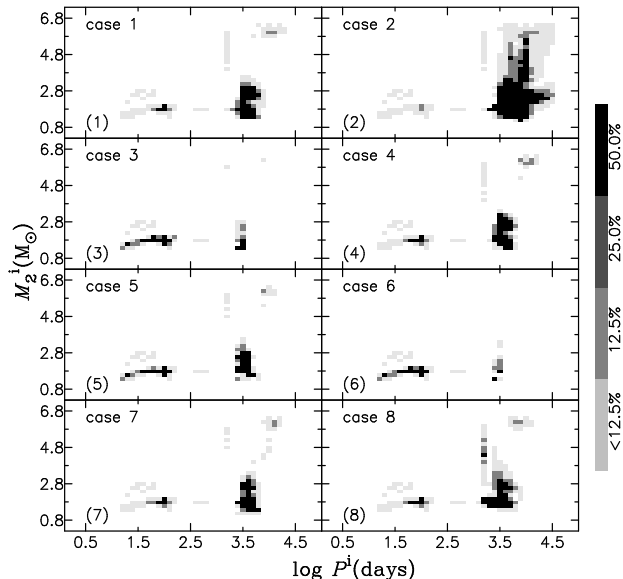


Figure 6. —Gray-scale maps of secondary initial masses M_2^i vs. initial orbital period P^i distribution for the progenitors of SNe Ia. The gradations of gray-scale correspond to the regions where the number density of systems is, respectively, within $1 - 1/2$, $1/2 - 1/4$, $1/4 - 1/8$, $1/8 - 0$ of the maximum of $\frac{\partial^2 N}{\partial \log P_i \partial \log M_i}$, and blank regions do not contain any stars. The cases shown in particular panels are indicated in their left-up corners.

2003). The evolutionary origin of SN 2002ic has been investigated by Livio & Reiss (2003) on the basis of a common envelope evolution model, by Han & Podsiadlowski (2006) on the basis of the delayed dynamical instability model of binary mass transfer, by Wood-Vasey & Sokolowski (2006) on the basis of a recurrent nova model with a RG, by Hachisu et al. (2008a) on the efficient mass-stripping from the companion star by the WD wind. Spectropolarimetry observations suggest that SN 2002ic exploded inside a dense, clumpy CS environment, quite possibly with a disk-like geometry (Wang et al. 2004). Subaru spectroscopic observations also provide evidence for an interaction of SN ejecta with a hydrogen-rich aspherical CS medium (Deng et al. 2004).

According to the above descriptions, the progenitor of SN 2002ic should have a large amount of CS material which has a disk-like geometry. In our model, the mass of the CS material is approximately calculated by

$$M_{CS} \approx \frac{D}{v_w^d} \eta \dot{M}_L + \frac{D}{v_w^s} (1 - \eta) \dot{M}_L - \Delta M_{WD} \quad (17)$$

where D is a distance from SN Ia, ΔM_{WD} is the increasing mass of WD for a span of $\frac{D}{v_w^d}$, v_w^d and v_w^s are the outflow velocity of the equatorial disk and spherical stellar wind, respectively. By assuming that SN Ia explodes inside a spherically symmetric CS envelope, Chugai & Yungelson (2004) estimated the total mass of the CS material for SN 2002ic is about $0.4 M_\odot$ within a radius of about 7×10^{15} cm, and for SN 1997cy about $6 M_\odot$ within a radius of about 2×10^{16} cm. Wang et al. (2004) suggested that there are several solar masses of material asymmetrically arrayed to distances of $\sim 3 \times 10^{17}$ cm. Therefore, we select the progenitor of SN 2002ic by two conditions: (i) the mass of CS material calcu-

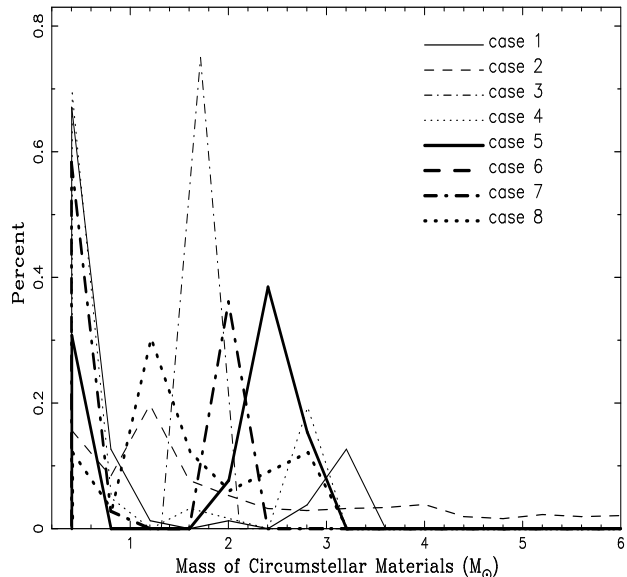


Figure 7. —The distribution of total masses of CS material for SN 2002ic (the number in every case is normalized to 1 and the width of the bin is $0.4 M_\odot$). The total masses of CS material is give by Eq. (17) in which D is 1×10^{17} cm.

lated by Eq. (17) being larger than $0.4 M_\odot$ within a radius of 10^{17} cm; (ii) a CS with a disk-like geometry which can interact with the ejecta of SN 2002ic. In our model there is always an equatorial disk around the secondary before it overflows its Roche lobe.

In Fig. 7, we give the distribution of total masses of CS material for SNe Ia like 2002ic within a radius of 10^{17} cm. The majority of the CS material lies in the orbital plane. Fig. 8 shows gray-scale maps of initial secondary masses M_2 vs. initial orbital period P distribution for the progenitors of SN 2002ic. In our model, the mass of CS material depends on the initial secondary mass. For examples, there are two peaks in Fig. 7 and two regions in Fig. 8 for case 1. The left peak around $\sim 0.6 M_\odot$ in Fig. 7 originates from the low region in Fig. 8, and the right peak around $\sim 0.6 M_\odot$ in Fig. 7 from the up region in Fig. 8.

SN 2002ic appeared to be a normal SN Ia from ~ 5 to 20 days after explosion (Wood-Vasey 2002; Hamuy et al. 2003), and brightened to twice the luminosity of a normal SN Ia and showed strong H_α emission around 22 days after explosion (Hamuy et al. 2003). The standard brightness during the first 20 days after explosion and the suddenness of the brightness around 22 days implied that the original SN explosion expanded into a region with little CS material, and then encountered a region with significant CS material (Wood-Vasey & Sokolowski 2006). Investigating the high-resolution optical spectroscopy at 256 d and HK-band infrared photometry at +278 and +380 d, Kotak et al. (2004) suggested that there is a dense and slow-moving ($\sim 100 \text{ km s}^{-1}$) outflow, and a dusty CS material in SN 2002ic. In our model, a cavity with little CS material around the accreting WD results from the WD's accretion, the dense and slow-moving outflow originates from the dense equatorial disk which have collided with the ejecta from SN explosion, and dust in CS material is formed in the dense equatorial disk. The radius of the cavity is roughly equal to the Roche

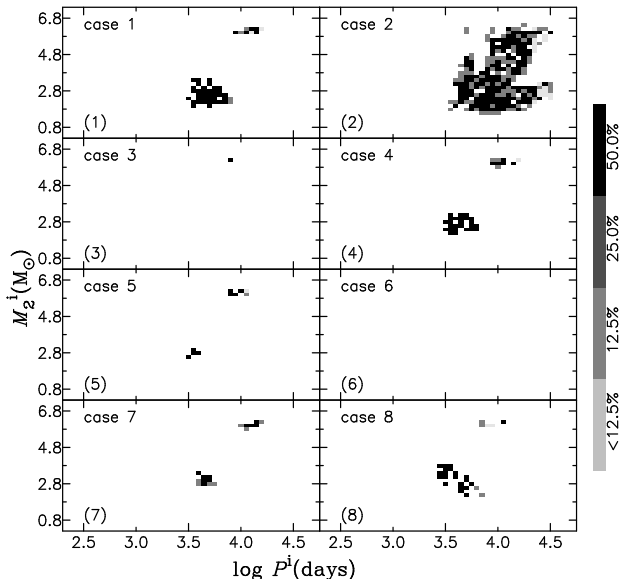


Figure 8. —Similar to Fig. 6, but for Gray-scale maps of initial secondary masses M_2 vs. initial orbital period P distribution for the progenitors of SN 2002ic.

lobe radius of the accreting WD, R_{L1} . The region out of the cavity has large amount of CS material which mainly originates from the equatorial disk. Due to orbital movement, the CS material out of the cavity has complicated structure. However, the most dense region lies on the equatorial disk around the secondary. The region where the ejecta from SN 2002ic firstly encountered the significant CS material is between R_{L1} and binary separation. Fig. 9 shows the distributions of R_{L1} and the binary separation of the progenitors of SN 2002ic prior to their explosion as a SN Ia. The observationally estimated region is $\sim 2 \times 10^{15}$ cm away from the explosion. Obviously, the majority of binary separations in our work are shorter than 2×10^{15} cm. A few binary separations in case 2 in which the equatorial disk has a low outflow velocity are longer than 2×10^{15} cm. As mentioned in §2.1, we do not consider an extended zone above the AGB star, which results in the underestimate for contribution of the symbiotic stars with long orbital periods to SN Ia.

We calculate the birthrates of SNe Ia like SN 2002ic in the Galaxy. From cases 1 to 8, they are 4.0×10^{-6} , 3.1×10^{-5} , 2.0×10^{-7} , 3.1×10^{-6} , 6.5×10^{-7} , ~ 0.0 , 1.8×10^{-6} and $1.6 \times 10^{-6} \text{ yr}^{-1}$, respectively. Compared with $3\text{--}4 \times 10^{-3} \text{ yr}^{-1}$ which is the birthrates of SNe Ia observationally estimated in the Galaxy, the birthrates of SNe Ia like SN 2002ic in this work are not more than 1% of the total birthrates of SNe Ia. SN 2002ic is very rare event in the Galaxy.

4.5 Progenitor of SN 2006X

Patat et al. (2007) detected the CS material in SN 2006X from variable Na I D (However, see Chugai (2008)). They found relatively low expansion velocities (Mean velocity is about $\sim 50 \text{ km s}^{-1}$), and estimated that the absorbing dust is a few 10^{16} cm from the SN. A possible interpretation given by Patat et al. (2007) is that the high-velocity ejecta of nova bursts in the progenitors are, by sweeping up the stellar wind of the donor star, slowed down to relatively low expansion

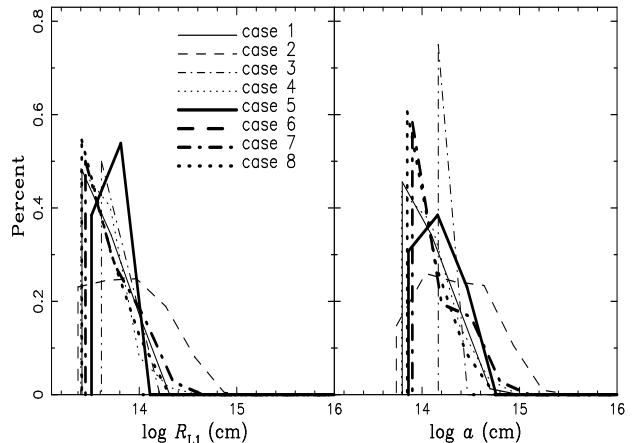


Figure 9. —Distributions of the Roche lobe radius of the accreting WD (R_{L1}) and the binary separation of the progenitors of SN 2002ic prior to their explosion as a SN Ia. The left and right panels are for Roche lobe radii of the accreting WDs and the binary separations, respectively.

velocities. According to the resolved light echo, Wang et al. (2008b) found that the illuminated dust is $\sim 27\text{--}170$ pc. The dust surrounding SN 2006X has multiple shells (Wang et al. 2008b), and stems from the progenitor. In addition, the dust surrounding SN 2006X is quite different from that observed in the Galaxy, and has a much smaller grain size than that of typical interstellar dust (Wang et al. 2008a,b).

Surprisingly, there is apparent presence of dust in the CS environment in the 2006 outburst of recurrent nova RS Oph (O’Brien et al. 2006; Bode et al. 2007). Evans et al. (2007) and Barry et al. (2008) reported that the dust appears to be present in the intervals of outbursts and is not created during the outburst event. This means that there is a dense region of the wind from the RG so that the dust can be formed (Bode et al. 2007). According to O’Brien et al. (2006) and Bode et al. (2007), the densest parts of the red-giant wind lie in the equatorial regions along the plane of the binary orbit. The dust in recurrent nova RS Oph originates possibly from the dense equatorial disk around the RG.

Therefore, it is possible that the progenitor of SN 2006X is very similar with recurrent nova RS Oph. We assume that the candidates for the progenitor of SN 2006X satisfy with following two conditions: (i) there is a dense equatorial disk around RG, which can produce dust; (ii) the progenitor of SN 2006X has undergone a series of weak thermonuclear outbursts presented by the filled triangles in Fig. 1 prior to explosion as SN Ia¹. The high-velocity ejecta from every thermonuclear outburst blow off the parts of the stellar wind including the dust produced by dense equatorial disk. During this process, the high-velocity ejecta are slowed down, and the dust can be irradiated so that the grain size becomes

¹ The thermonuclear outburst in this work has an ejecta without an increase of CO WD’s mass (strong hydrogen-shell burning), or has an increase of CO WD’s mass without an ejecta (mildly hydrogen-shell burning). However, according to Yaron et al. (2005), there is some material ejected during a mildly hydrogen-shell burning. We assume that the progenitor of SN 2006X has undergone a mildly hydrogen-shell burning.

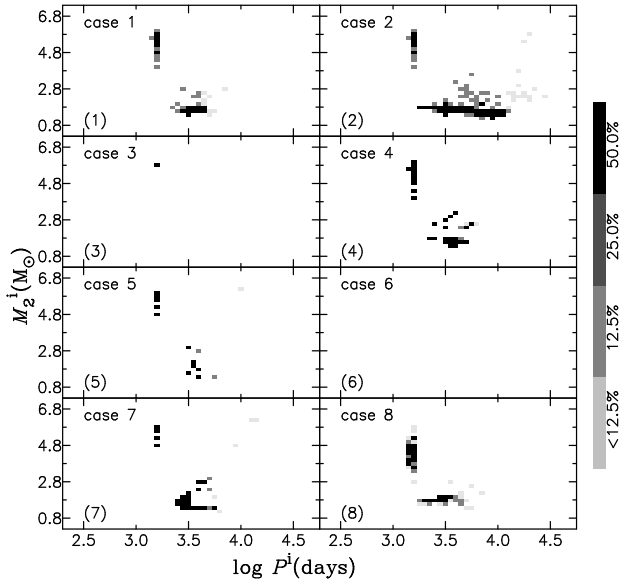


Figure 10. —Similar to Fig. 6, but for progenitors of SN 2006X.

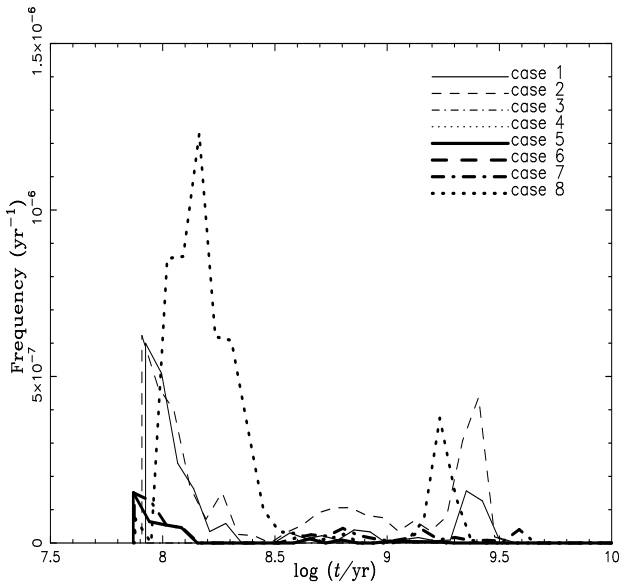


Figure 11. —Similar to Fig. 3, but for progenitors of SN 2006X.

small. A more detailed model for SN 2006X is in preparation.

According to the above conditions, we select the possible progenitors of SN 2006X from our sample which are showed in Fig. 10. The birthrates of SNe Ia like SN 2006X in the Galaxy from cases 1 to 8 are 9.3×10^{-6} , 2.5×10^{-5} , 1.0×10^{-7} , 6.3×10^{-6} , 1.2×10^{-6} , ~ 0.0 , 3.8×10^{-6} and $7.0 \times 10^{-6} \text{ yr}^{-1}$, respectively. Therefore, SNe Ia like SN 2006X are very rare events. Fig. 11 displays the evolution of birthrates of SNe Ia like SN 2006X for a single star burst.

5 CONCLUSION

By a toy model in which the cool giant in symbiotic star has an aspherical stellar wind with an equatorial disk, we inves-

tigate the production of SNe Ia via symbiotic channel. We estimate that the Galactic birthrate of SNe Ia via symbiotic channel is between 1.03×10^{-3} (case 2) and $2.27 \times 10^{-5} \text{ yr}^{-1}$ (case 6), the delay time of SNe Ia has wide range from ~ 0.07 to 5 Gyr. The results are greatly affected by the outflow velocity and mass-loss rate of the equatorial disk. The progenitor of SN 2002ic may be a WD+RG in which there is a dense equatorial disk around the RG. The CS environment of SN 2002ic may mainly originate from the dense equatorial disk. In the progenitor of SN 2006X, the CO WD has undergone a series of mildly unstable hydrogen-shell burning, and the dust in the CS environment may originate from a dense equatorial disk around the RG and is swept out by the ejecta of every thermonuclear outburst.

ACKNOWLEDGMENTS

We are grateful to the referee, N. Soker, for careful reading of the paper and constructive criticism. We thank Zhanwen Han for some helpful suggestions. This work was supported by National Science Foundation of China (Grants Nos. 10647003 and 10763001) and National Basic Research Program of China (973 Program 2009CB824800).

REFERENCES

- Asida S. M., Tuchman Y., 1995, *ApJ*, 455, 286
- Balick B., 1987, *AJ*, 94, 671
- Barry B. K. et al., 2008, *ApJ*, 677, 1253
- Bjorkman J. E., Cassinelli J. P., 1993, *ApJ*, 409, 429
- Bode M. F., Harman D. J., O'Brien T. J., Bond H. E., Starrfield S., Darnley M. J., Evans A., Eyres E. P. S., 2007, *ApJL*, 665, 63
- Boffin H. M. J., Jorissen A., 1988, *A&A*, 205, 155
- Bondi H., Hoyle F., 1944, *MNRAS*, 104, 273
- Cappellaro E., Turatto M., 1997 in Ruiz-Lapuente, P., Canal, R., & Isern J., eds, *Thermonuclear Supernovae* (Kluwer, Dordrecht), P. 77
- Chen W. C., Li X. D., 2007, *ApJ*, 658, L51
- Chen X. F., Han Z., 2008, *MNRAS*, 387, 1416
- Chugai N. N., Yungelson L. R., 2004, *Astronomy Letters*, 30, 65
- Chugai N. N., 2008, *Astronomy Letters*, 34, 389
- Deng J. et al., 2004, *ApJ*, 605, L37
- Eggleton P. P., Fitchett M. J., Tout C. A., 1989, *ApJ*, 347, 998
- Evans A. et al., 2007, *ApJL*, 671, 157
- Frank A., 1999, *NewA Rev.*, 43, 31
- Frankowski A., Tylenda R., 2001, *A&A*, 367, 513
- Hachisu I., Kato M., Nomoto K., 1996, *ApJL*, 470, 97
- Hachisu I., Kato M., Nomoto K., 1999, *ApJ*, 522, 487
- Hachisu I., Kato M., Nomoto K., 2008a, *ApJ*, 679, 1390
- Hachisu I., Kato M., Nomoto K., 2008b, *ApJ*, 683, 127
- Hamuy M. et al., 2003, *Nat.*, 424, 651
- Han Z., Eggleton P. P., Podsiadlowski Ph., Tout C. A., 1995, *MNRAS*, 272, 800
- Han Z., Eggleton P. P., Podsiadlowski Ph., Tout C. A., Webbink R. F., 2001, in Podsiadlowski Ph., Rappaport S., King A. R., D'Antona F., Burderi L., eds, *Evolution*

- of Binary and Multiple Star Systems, ASP Conf. Ser., Vol. 229, p. 205
- Han Z., Podsiadlowski, Ph., Maxted P. F. L., Marsh T. R., Ivanova N., 2002, MNRAS, 336, 449
- Han Z., Podsiadlowski Ph., 2004, MNRAS, 350, 1301
- Han Z., Podsiadlowski Ph., 2006, MNRAS, 368, 1095
- Hjellming M. S., Webbink R. F., 1987, ApJ, 318, 794
- Hurley J. R., Pols O. R., Tout C. A., 2000, MNRAS, 315, 543
- Hurley J. R., Tout C. A., Pols R., 2002, MNRAS, 329, 897
- Kato M., Hachisu I., 2004, ApJ, 613, L129
- Kato M., Hachisu I., Kiyota S., Saio H., 2008, ApJ, 684, 1366
- Kenyon S. J., Fernandez-Castro T., Stencel R. E., 1988, AJ, 95, 1817
- Kotak R., Meikle W. P. S., Adamson A., Leggett S. K., 2004, MNRAS, 354, L13
- Li X. D., van den Heuvel E. P. J., 1997, A&A, 322, L9
- Livio M., Reiss A. G., 2003, ApJ, 594, L93
- Lü G. L., Yungelson L., Han Z., 2006, MNRAS, 372, 1389
- Lü G. L., Zhu C. H., Han Z., Wang Z. J., 2008, ApJ, 683, 990
- Mannucci F., Della Valle M., Panagia N., 2006, MNRAS, 370, 773
- Marion G. H., Höflich P., Vacca W. D., Wheeler J. C., 2003, ApJ, 591, 316
- Matt S., Balick B., Winglee R., Goodson A., 2000, ApJ, 545, 965
- Mattila S., Lundqvist P., Sollerman J., Kozma C., Baron E., Fransson C., Leibundgut B., Nomoto K., 2005, A&A, 443, 649
- Mazeh T., Goldberg D., Duquennoy A., Mayor M., 1992, ApJ, 401, 265
- Meng X. C., Chen X. F., Han Z., 2008, MNRAS, in press(arXiv:0802.2471)
- Miller G. E., Scalo J. M., 1979, ApJS, 41, 513
- Mikołajewska J., Ivison R. J., Omont A., 2003, Edited by Corradi R. L. M., Mikołajewska R., Mahoney T. J., Symbiotic Stars Probing Stellar Evolution, ASP Conference Proceedings, Vol. 303., p.478
- Nieuwenhuijzen H., de Jager C., 1988, A&A, 203, 355
- Nomoto K., Thielemann F., Yokoi K., 1984, ApJ, 286, 644
- Nomoto K., Iben I. Jr., 1985, ApJ, 297, 531
- O'Brien T. J. et al., 2006, Nat., 442, 279
- Patat E. et al. 2007, Science, 317, 924
- Perlmutter S. et al., 1999, ApJ, 517, 565
- Phillips J. P., 1989, in IAU Symp. 131, Planetary nebulae, ed. S. Torres-Peimbert, p.425
- Reimers D., 1975, Mem.Soc.R.Sci.Liege, 8, 369
- Riess A. et al., 1998, AJ, 116, 1009
- Saio H., Nomoto K., A&A, 150, L21
- Seaquist E. R., Krogulec M., Taylor A. R., 1993, ApJ, 410, 260
- Soker N., 1992, PASP, 104, 923
- Soker N., 1994, MNRAS, 270, 774
- Soker N., 1997, ApJS, 112, 487
- Soker N., Rappaport S., 2000, ApJ, 538, 241
- Soker N., 2002, MNRAS, 337, 1038
- Soker N., 2008, NewA, 13, 491
- van den Bergh S., Tammann G. A., 1991, ARA&A, 29, 363
- van den Heuvel E. P. J., Bhattacharya D., Nomoto K., Rappaport S., 1992, A&A, 262, 97
- Vassiliadis E., Wood P. R., 1993, ApJ, 413, 641
- Voss R., Nelemans G., 2008, Nat., 451, 802
- Wang B., Meng X., Chen X., Han Z., 2009, MNRAS, in press (arXiv:0901.3496)
- Wang L., Baade D., Höflich P., Wheeler C., Kawabata K., Nomoto K., 2004, ApJ, 604, L53
- Wang X. F. et al., 2008, ApJ, 675, 626
- Wang X. F., Li W. D., Filippenko A. V., Foley R. J., Smith N., Wang L., 2008, ApJ, 677, 1060
- Webbink R. F., 1988, in Mikołajewska J., Friedjung M., Kenyon S. J., Viotti R., eds, Proc. IAU Colloq. 103, The Symbiotic Phenomenon. Kluwer, Dordrecht, P.311
- Wood-vasey W. M., 2002, IAU Circ. 8019
- Wood-vasey W. M., Sokoloski J. L., 2006, ApJ, 645, L53
- Yaron O., Prialnik D., Kovetz A., 2005, ApJ, 623, 398
- Yungelson L., Tutukov A. V., Livio M., 1993, ApJ, 418, 794
- Yungelson L., Livio M., Tutukov A. V., Kenyon S. J., 1995, ApJ, 477, 656
- Yungelson L., Livio M., 1998, ApJ, 497, 168
- Zamanov R. K., Bode M. F., Melo C. H. F., Stateva I. K., Bachev R., Gomboc A., Konstantinova-Antova R., Stoyanov K. A., 2008, MNRAS, 390, 377
- Zhang F. H., Li L. F., Han Z., 2005, MNRAS, 364, 503
- Zuckerman B., Aller L. H., 1986, ApJ, 301,772

This paper has been typeset from a \TeX / \LaTeX file prepared by the author.